Parallel trapping of multiwalled carbon nanotubes with optoelectronic tweezers

Peter J. Pauzauskie,[1,a] Arash Jamshidi,[2] Justin K. Valley,[2] Joe H. Satcher, Jr.,[1] and Ming C. Wu[2,a]

[1]*Chemical Sciences Division, Lawrence Livermore National Laboratory, 7000 East Ave. L-231, Livermore, California 94551, USA*
[2]*Department of Electrical Engineering, University of California, Berkeley, Cory Hall, Berkeley, California 94720, USA*

Here we report the use of optoelectronic tweezers and dynamic virtual electrodes to address multiwalled carbon nanotubes (MWCNTs) with trap stiffness values of approximately 50 fN/μm. Both high-speed translation (>200 μm/s) of individual-MWCNTs and two-dimensional trapping of MWCNT ensembles are achieved using 100,000 times less optical power density than single beam laser tweezers. Modulating the virtual electrode's intensity enables tuning of the MWCNT ensemble's number density by an order of magnitude on the time scale of seconds promising a broad range of applications in MWCNT science and technology. © 2009 American Institute of Physics. [doi:10.1063/1.3212725]

Optoelectronic tweezers (OETs) have emerged recently as a massively parallel optical platform for trapping submicron scale particles.[1] The noncontact approach allows for thousands of individual traps to be created and controlled in two dimensions under a standard objective lens. To date, the technique has been used to manipulate living cells, polystyrene beads,[1,2] and solid-state nanowires[3] using $\sim 10^5$ times less optical power density than single-beam laser traps.[4]

Over the past two decades multiwalled carbon nanotubes (MWCNTs) have been employed in myriad applications including desalination membranes,[5] chemical sensors,[6] additives for high-strength polymer composites,[7] field emitters,[8] and integrated circuits.[9,10] Although an impressive degree of control has been achieved for MWCNT synthesis,[11] currently no optical method exists for freely trapping and translating individual MWCNTs in solution, with contemporary approaches typically relying on either dielectrophoresis (DEP) or single-beam laser tweezers. In DEP, lithographically patterned metallic electrodes have been demonstrated as a highly parallel approach for self-limiting, ultralarge-scale nanotube integration,[12] and separations[13] in two dimensions. However, the fixed metallic electrodes used in this method do not allow for dynamic translation of isolated structures. In contrast to DEP, laser tweezers[4] are the most common optical method for three-dimensional translation of single walled carbon nanotube (SWCNT) materials in solution with either single- or multiple- beam laser traps.[14–19]

When compared with SWCNTs, few optical methods exist for addressing MWCNTs due to their large diameters and corresponding metallic conductivity.[20] Detrimental heating arises within MWCNTs from free-carrier absorption of the intense laser trapping fields corresponding to what has been reported for metallic silver nanostructures.[21] OET is particularly well suited for trapping metallic MWCNTs given it can combine the massive parallelism of DEP with the optical flexibility of laser tweezers by using optical intensities low enough to minimize detrimental effects from MWCNT optical absorption.

OET works based on the principle of an optically induced DEP force. In this technique, optical images are projected onto the hydrogenated amorphous silicon (a-Si:H) at low irradiances ($\sim$5 nW/μm^2) creating electron-hole pairs where light is patterned [Fig. 1(a)]. Photoconductive gain
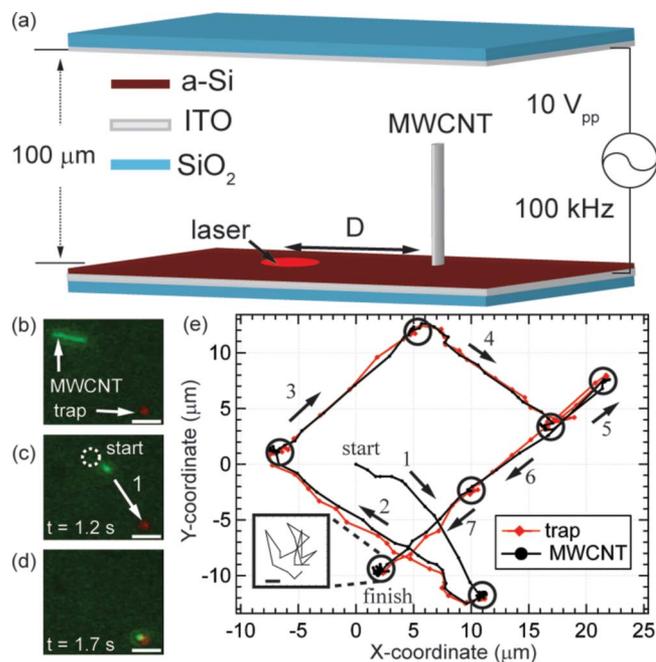
FIG. 1. (Color online) (a) OET chamber schematic. (b) Dark field image of an isolated MWCNT in Brownian motion. Scale bar −5 μm. (c) Alignment and initial translation of the MWCNT following 10 Vpp, 100 kHz field applied to chamber. (d) Translation over $\sim$15 μm of the MWCNT into the OET trap. (e) *X-Y* coordinates of MWCNT and trapping laser measured from video frames. Circles indicate locations where trapping laser was temporarily static. Inset: Coordinates of trapped MWCNT in static laser at finish. Scale bar −200 nm (enhanced online).

[URL: http://dx.doi.org/10.1063/1.3212725.1]
[URL: http://dx.doi.org/10.1063/1.3212725.2]

a)Authors to whom correspondence should be addressed. Electronic addresses: wu@eecs.berkeley.edu and pauzauskie1@llnl.gov.
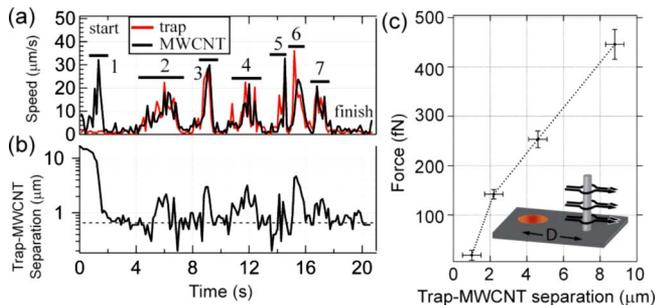
FIG. 2. (Color online) (a) Absolute speed and (b) absolute separation of MWCNT and laser during the course of the trapping measurement in Fig. 1. (c) Trapping stiffness measurement from force on MWCNT measured from Stokes drag exerted by the trapping laser during trace 1 in Fig. 1. Inset: schematic of fluid flow around MWCNT.

dramatically lowers the local impedance of the a-Si:H in the area that the laser is present, transferring voltage to the liquid layer and locally forming a nonuniform electric field in the liquid due to the applied ac bias. The nonuniform electric field present in the liquid layer attracts the polarized tubes to areas with the highest electric-field intensity-gradient according to classical DEP principles.

Single nanotube imaging employing either fluorescent labels[22] or intrinsic SWCNT photoluminescence[23] has been used recently to measure translational and rotational diffusion coefficient for individual SWCNT structures. Individual MWCNTs can be observed without fluorescent labeling due to their large Rayleigh scattering cross section using dark-field microscopy and either a color or electron-multiplying charge coupled device.[24] A large (80 nm diameter) multi-walled carbon nanofiber is shown in Fig. S1(c),[25] representing the upper bound of the MWCNT size used in this study. In solution, MWCNTs undergo Brownian motion before the trapping voltage is applied to the chamber [Fig. 1(b)]. Once the trapping voltage is applied to the OET device, the MWCNTs experience a torque aligning them with the electric field [Fig. 1(c), supporting video S1[25]] and a positive DEP force causing them to translate toward the OET laser trap [Fig. 1(d)], analogous to what has been reported for silver nanowires.[3]

The MWCNT is observed to follow the laser trap as it translates throughout the OET device. Discrete translation events are labeled in Fig. 1(e) by a Roman numeral with an arrow indicating the direction of motion. Circled regions indicate where the laser trap was brought to momentary rest. For the first MWCNT translation, the laser is stationary and the MWCNT moves into the trap after the ac field is applied across the indium tin oxide electrodes. The trap is then translated by hand through a diamond shaped course filling a region of approximately 100 μm² before it is brought to rest. When the trapping spot is stationary, the MWCNT is confined to a region less than 1 μm² [Fig. 1(e), inset] while continuing to undergo Brownian motion.

The respective position coordinates for the MWCNT and trapping laser spot can be analyzed further to gain information on the absolute speed of the MWCNT and trap, as well as their relative separation. Figure 2(a) shows the instantaneous speeds for both the MWCNT and trapping laser over the course of approximately 20 s while Fig. 2(b) shows their relative separation. During trace 1 (when the laser velocity is zero), the tube velocity exceeds 30 μm/s as it translates into

the trapping laser. The trap is then translated through traces 2–7, and the MWCNT's velocity is observed to respond after each translation event.

Inertial forces are negligible in the trap as a consequence of the extremely small Reynolds number that exists at the operating conditions of this device (Re $\sim 10^{-6}$). Therefore, MWCNT motion is dominated by a competition between OET forces, Brownian motion, and viscous drag. Due to their large aspect ratios and the variable shape of their end facets, we model the MWCNTs as elongated, prolate ellipsoids, with the lateral hydrodynamic drag force given by[26]

$$|\vec{F}_{\text{drag}}| \approx \frac{8\pi\eta L}{2\,\ln(2L/d)+1}\cdot|\vec{v}|,$$

where η is the viscosity of water, L and d are the MWCNT's length and diameter, respectively, v the MWCNT velocity, and F_{drag} is the laminar drag force on the translating MWCNT. By neglecting end-facet dissipation, this calculation provides a conservative lower-bound measure of applied forces that are approximately 10% lower than for a circular cylinder[27] with an equivalent aspect ratio. In Fig. 2(c) we plot the calculated force as a function of absolute MWCNT-trap separation using the measured MWCNT length of ~ 6 μm and the upper-bound diameter of 80 nm for the sample of MWCNTs. This results in an approximately linear response as the MWCNT moves into the stationary laser trap over a distance of ~ 10 μm. A linear fit to this region of data reveals an approximate trap stiffness of 50 fN/μm, corresponding to OET-trap stiffness values that have been reported for inorganic nanowires.[3] Additional experiments with a motorized translation stage (Newport) have shown MWCNTs to move with speeds of 235 ± 29 μm/s (supporting video S2[25]), which is in agreement with calculated trapping forces on the order of piconewtons.

Many postsynthetic processing techniques such as selective surface binding,[28] inkjet printing,[29] or microcontact stamps[30] operate on large ensembles of nanotubes. Consequently, parallel MWCNT processing with OET requires investigation of the case when multiple MWCNTs are trapped simultaneously in a virtual electrode. Figures 3(a) and 3(b) show dark-field images of the two MWCNTs trapped together in a common virtual electrode, as well as the MWCNTs in Brownian motion after the trapping voltage is turned off [Fig. 3(c)]. The Brownian motion of the tubes shown in Fig. 3(d) differs significantly from that of a single trapped MWCNT [Fig. 1(e), inset] in that the pair of tubes are not free to move across the OET virtual electrode, but rather occupy separate sides due to mutual repulsion from in-phase induced dipole moments. Figure 3(e) shows the histogram of tube-tube separation with the mean separation of the tubes measured to be roughly 3 μm, consistent with the size of the trapping spot.

This observed mutual dipole-dipole repulsion can be used for modulating the number density of MWCNTs in the OET device simply by actuating the virtual electrode. In Fig. 3(f), measurements are made on the number density of >15 MWCNTs in a ~ 10 μm OET trapping spot. By turning on the trapping spot, all tubes are collected in the virtual electrode, with a number density of approximately 0.2 MWCNTs/μm². When the laser is removed, the tubes experience an immediate dipole-induced repulsion, with an exponentially decaying number density that reaches a base-
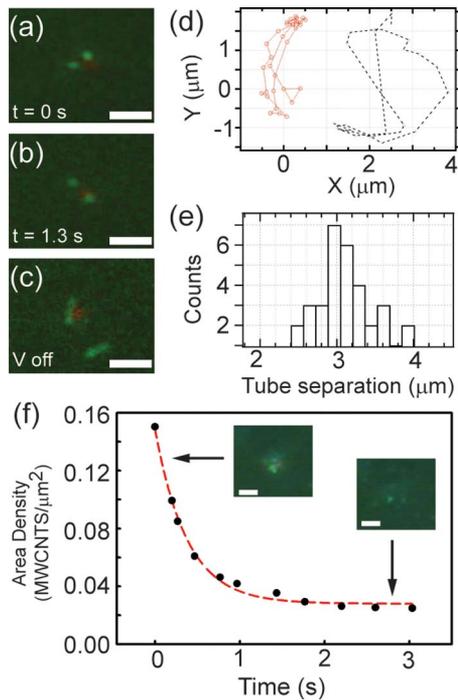
FIG. 3. (Color online) [(a)–(b)] Dark-field microscope images of two MWCNTs trapped in a single OET virtual electrode at different times with voltage on. Scale bar −5 μm. (c) Corresponding MWCNTs with voltage off. (d) The Brownian motion trajectory of the tubes inside the trap, occupying separate sides of the trap from dipole-dipole interaction. (e) Histogram of tube-tube separation. (f) Number density of >15 MWCNTs in a ~10 μm OET trapping spot before and after trapping laser is turned off. Insets show dark-field images corresponding to when the OET laser is on and off. Scale bar −5 μm.

line value of 0.02 MWCNTs/μm^2 in approximately 3 s. This number density is still two orders of magnitude below what has been achieved with high-density MWCNT synthesis[5] but represents a rapid optical method for locally tuning the density of MWCNTs over an order of magnitude.

In conclusion, we have demonstrated that both individual and multiple MWCNTs can be translated and positioned in solution with OET. Optical control of MWCNT density offers a potential means to tune electrical, thermal, optical, and mass transport properties in MWCNT-composite thin films, expanding possibilities for device fabrication.

[1]P. Y. Chiou, A. T. Ohta, and M. C. Wu, Nature (London) **436**, 370 (2005).
[2]A. T. Ohta, P. Y. Chiou, T. H. Han, J. C. Liao, U. Bhardwaj, E. R. B. McCabe, F. Q. Yu, R. Sun, and M. C. Wu, J. Microelectromech. Syst. **16**, 491 (2007).
[3]A. Jamshidi, P. J. Pauzauskie, P. J. Schuck, A. T. Ohta, P. Y. Chiou, J. Chou, P. D. Yang, and M. C. Wu, Nat. Photonics **2**, 86 (2008).
[4]D. G. Grier, Nature (London) **424**, 810 (2003).
[5]B. J. Hinds, N. Chopra, T. Rantell, R. Andrews, V. Gavalas, and L. G. Bachas, Science **303**, 62 (2004).
[6]C. Y. Lee, R. Sharma, A. D. Radadia, R. I. Masel, and M. S. Strano, Angew. Chem., Int. Ed. **47**, 5018 (2008).
[7]L. Ci, J. Suhr, V. Pushparaj, X. Zhang, and P. M. Ajayan, Nano Lett. **8**, 2762 (2008).
[8]S. T. Purcell, P. Vincent, C. Journet, and V. T. Binh, Phys. Rev. Lett. **88**, 105502 (2002).
[9]B. Q. Wei, R. Vajtai, and P. M. Ajayan, Appl. Phys. Lett. **79**, 1172 (2001).
[10]A. Javey, J. Guo, Q. Wang, M. Lundstrom, and H. J. Dai, Nature (London) **424**, 654 (2003).
[11]N. Halonen, K. Kordas, G. Toth, T. Mustonen, J. Maklin, J. Vahakangas, P. M. Ajayan, and R. Vajtai, J. Phys. Chem. C **112**, 6723 (2008).
[12]A. Vijayaraghavan, S. Blatt, D. Weissenberger, M. Oron-Carl, F. Hennrich, D. Gerthsen, H. Hahn, and R. Krupke, Nano Lett. **7**, 1556 (2007).
[13]R. Krupke, F. Hennrich, H. von Lohneysen, and M. M. Kappes, Science **301**, 344 (2003).
[14]J. Plewa, E. Tanner, D. M. Mueth, and D. G. Grier, Opt. Express **12**, 1978 (2004).
[15]O. M. Marago, P. H. Jones, F. Bonaccorso, V. Scardaci, P. G. Gucciardi, A. G. Rozhin, and A. C. Ferrari, Nano Lett. **8**, 3211 (2008).
[16]F. Borghese, P. Denti, R. Saija, M. A. Iati, and O. M. Marago, Phys. Rev. Lett. **100**, 163903 (2008).
[17]J. Zhang, H. I. Kim, C. H. Oh, X. D. Sun, and H. Lee, Appl. Phys. Lett. **88**, 053123 (2006).
[18]S. D. Tan, H. A. Lopez, C. W. Cai, and Y. G. Zhang, Nano Lett. **4**, 1415 (2004).
[19]T. Rodgers, S. Shoji, Z. Sekkat, and S. Kawata, Phys. Rev. Lett. **101**, 127402 (2008).
[20]Y. Ando, X. Zhao, H. Shimoyama, G. Sakai, and K. Kaneto, Int. J. Inorg. Mater. **1**, 77 (1999).
[21]P. J. Pauzauskie, A. Radenovic, E. Trepagnier, H. Shroff, P. D. Yang, and J. Liphardt, Nature Mater. **5**, 97 (2006).
[22]R. Duggal and M. Pasquali, Phys. Rev. Lett. **96**, 246104 (2006).
[23]D. A. Tsyboulski, S. M. Bachilo, A. B. Kolomeisky, and R. B. Weisman, ACS Nano **2**, 1770 (2008).
[24]Z. H. Yu and L. Brus, J. Phys. Chem. B **105**, 1123 (2001).
[25]See EPAPS supplementary material at http://dx.doi.org/10.1063/1.3212725 for experimental details, digital video of MWCNT trapping, and finite-element simulations.
[26]J. Happel and H. Brenner, *Low Reynolds Number Hydrodynamics* (Kluwer Academic, Boston, 1991).
[27]S. Broersma, J. Chem. Phys. **74**, 6989 (1981).
[28]M. C. LeMieux, M. Roberts, S. Barman, Y. W. Jin, J. M. Kim, and Z. N. Bao, Science **321**, 101 (2008).
[29]K. Kordas, T. Mustonen, G. Toth, H. Jantunen, M. Lajunen, C. Soldano, S. Talapatra, S. Kar, R. Vajtai, and P. M. Ajayan, Small **2**, 1021 (2006).
[30]Q. Cao, H. S. Kim, N. Pimparkar, J. P. Kulkarni, C. J. Wang, M. Shim, K. Roy, M. A. Alam, and J. A. Rogers, Nature (London) **454**, 495 (2008).